Analytical results and feedback circuit analysis for simple chaotic flows

2003 J. Phys. A: Math. Gen. 36 11229

(http://iopscience.iop.org/0305-4470/36/44/004)

INSTITUTE OF PHYSICS PUBLISHING JOURNAL OF PHYSICS A: MATHEMATICAL AND GENERAL

J. Phys. A: Math. Gen. **36** (2003) 11229–11245 PII: S0305-4470(03)58749-2

Analytical results and feedback circuit analysis for simple chaotic flows

Christophe Letellier[1] **and Olivier Vallée**[2]

[1] CORIA UMR 6614—Université de Rouen, Av. de l'Université, BP 12, F-76801 Saint-Etienne du Rouvray Cedex, France
[2] Laboratoire d'Analyse Spectroscopique et d'Energétique des Plasmas—UPRES EA 3269, Université d'Orléans, Rue Gaston Berger, BP 4043, F-18028 Bourges Cedex, France

Received 21 January 2003, in final form 5 August 2003
Published 22 October 2003
Online at stacks.iop.org/JPhysA/36/11229

Abstract
Simple jerk systems are very useful for combining analytical computations and dynamical analysis in phase space. This is particularly relevant since there is still no direct link between the algebraic structure of ordinary differential equations and the topology of the chaotic attractors which they generate. In this paper, particular analytical solutions are identified for three simple chaotic flows. It is shown that these solutions have varying effects on the bifurcation diagrams. Moreover, a feedback circuit analysis is used to exhibit the similarities between the three simple systems. Such analysis also exhibits the relevant role of double nullcline in the topology of the attractor.

PACS number: 05.45.+b

1. Introduction

In investigating the restricted three-body problem, Poincaré showed that no general analytical solution can be found [1]. In addition, he showed that the behaviour is very sensitive to initial conditions. In a modern language, the Poincaré–Bendixson theorem [2] requires that autonomous first-order ordinary differential equations with continuous functions have to be at least three dimensional to have bounded chaotic solutions. During his search for a simple system displaying both sensitivity to initial conditions as well as long-term instability, Lorenz discovered a set of three ordinary differential equations derived from the hydrodynamical equations describing a Rayleigh–Bénard convection [3]. Rössler later simplified the Lorenz equations by removing the symmetry of the system. He obtained a simple chaotic band attractor [4] generated by a set of three ordinary differential equations which are algebraically simpler than the Lorenz equations. The equations are constituted by seven terms with a single quadratic nonlinearity unlike the two observed in the Lorenz system. In 1979, Rössler [5] found a toroidal chaotic system with six terms and one quadratic nonlinearity.

An extensive computer search by Sprott revealed 14 additional chaotic systems including six terms and one quadratic nonlinearity, as well as five systems with five terms and two quadratic nonlinearities [6]. Gottlieb [7] then noted that some of the equations for the new found systems could be rewritten as a single third-order differential equation. Prior to Gottlieb, it was shown by Gouesbet and Letellier while investigating global modelling techniques [8] that the Lorenz and the Rössler systems can be rewritten in such a form but with rational functions. Note the exception of the Rössler system when it is rewritten in such a form from the y-variable: in this case, the function is a polynomial. This was also done later by Linz [9]. Fu and Heidel [10] showed that quadratic functions with fewer than three terms cannot be chaotic. More recently, Malasoma proposed the simplest chaotic jerk equations which have symmetry properties [11].

A search for such simple equations generating chaotic behaviour is very useful for developing analytical manipulations and, consequently, to propose a link between the algebraic structure of the ordinary differential equations and the type of chaotic behaviour they induce. In this paper, three simple chaotic systems which may be written under the form of a jerk system will be investigated. It will be shown that particular solutions with an explicit algebraic form may be found. These solutions have a preponderant role in limiting the control parameter range over which a chaotic attractor may be observed. In addition, a feedback circuit analysis introduced by Thomas [12] will be proposed to exhibit the roots of the equivalence between these three systems. The subsequent part of this paper is organized as follows. Section 2 will describe briefly the principle of the feedback circuit analysis. In section 3, three simple jerk systems will be investigated and section 4 gives a conclusion.

2. Feedback circuit analysis

The ideas of feedback circuits were developed in the context described by Boolean logic, or dynamical systems with linear step-function dynamics (or sigmoidal functions with high Hill number) [13, 14]. More recently, such an analysis was extended to more general dynamical systems [14, 15]. It provides a first link between the algebraic structure of the ordinary differential equations and their asymptotic behaviour. This results from the fact that feedback circuits can be associated with fixed points which structure the phase portrait [16]. Thus, feedback circuits can serve as a qualitative guide to interpret differential equations although they give no information on the bifurcation diagram.

For the dynamical system

$$\dot{x}_i = f_i(x_1, x_2, x_3) \qquad (i = 1, 2, 3) \tag{1}$$

described in a three-dimensional phase space for the sake of simplicity, there are some interactions between the dynamical variables x_i which can be defined using the elements of the Jacobian matrix. Variable x_j acts on variable x_i if the term J_{ij} of the Jacobian matrix is non-zero. This action is positive or negative depending on the sign of element J_{ij}. A full circuit is defined as a sequence of non-zero elements in the Jacobian matrix corresponding to one of the products appearing in the analytic expression of the determinant of the Jacobian matrix. For a three-dimensional system,

$$\mathrm{Det}(\mathcal{J}) = J_{11}J_{22}J_{33} - J_{11}J_{23}J_{32} - J_{22}J_{31}J_{13} - J_{33}J_{12}J_{21} + J_{12}J_{23}J_{31} + J_{13}J_{32}J_{21} \tag{2}$$

up to six full circuits may be identified. A feedback circuit is positive or negative depending on the parity of negative elements, J_{ij}, in these products. Partial feedback circuits which do not involve all dynamical variables are also of interest. Thus, for three-dimensional systems, a partial circuit is defined by a two-element product $J_{ij}J_{ji}$ $(i \neq j)$ or by a single element J_{kk}.

The six full circuits identified for three-dimensional systems can be classified in two groups. The first group is decomposable while the second is not.

- *Decomposable*. The full circuit is the union of partial circuits. It may be either the union of one two-element circuit $J_{ij}J_{ji}$ ($i \neq j$) and one 'single-element circuit' J_{kk} ($k \neq i$ and $k \neq j$), or the union of three 'one-element circuits'.
- *Indecomposable*. The full circuit cannot be decomposed into the union of partial circuits.

For a three-dimensional system, we therefore have four decomposable circuits ($J_{11}J_{22}J_{33}$, $J_{11}J_{23}J_{32}$, $J_{22}J_{31}J_{13}$ and $J_{33}J_{12}J_{21}$) and two indecomposable circuits ($J_{12}J_{23}J_{31}$ and $J_{13}J_{32}J_{21}$).

It has been shown in the context of logical description [17] that feedback circuits can be functional or not depending whether they are responsible for the existence of a fixed point. Indeed, each full circuit, when isolated, can generate one or more fixed points. To generate a given fixed point, the eigenvalues of the Jacobian matrix only retaining the elements of the isolated full circuits must be of the same nature as those of the given fixed point for the whole system. To be explicit, the two indecomposable full circuits, $J_{12}J_{23}J_{31}$ and $J_{13}J_{32}J_{21}$, are associated with eigenvalues $\lambda_k = \sqrt[3]{J_{12}J_{23}J_{31}}$ and $\lambda_k = \sqrt[3]{J_{13}J_{32}J_{21}}$, respectively. They can therefore generate only saddle-focii, of type SF_+ (one positive real eigenvalue and a pair of complex conjugate eigenvalues with negative real parts) when $J_{ij}J_{jk}J_{ki} > 0$, or SF_- (one negative real eigenvalue and two complex conjugate eigenvalues with positive real parts) when $J_{ij}J_{jk}J_{ki} < 0$. The three decomposable full circuits $J_{ij}J_{ji}J_{kk}$ have eigenvalues computed using elements J_{ij}, J_{ji} and J_{kk} completed by the diagonal elements J_{ii} and J_{jj}. These eigenvalues are

$$\lambda_{1,2} = \frac{(J_{ii} + J_{jj}) \pm \sqrt{(J_{ii} - J_{jj})^2 + 4J_{ij}J_{ji}}}{2}. \tag{3}$$

In the case above, the associated fixed point can be a node, a node-focus, a saddle-focus (SF_+ or SF_-) or a saddle. In the case of circuit $J_{ii}J_{jj}J_{kk}$, the eigenvalues are the diagonal elements themselves. All these elements are real and the associated fixed point is a node or a saddle point.

When the system is linear, all the elements of the Jacobian matrix are constant and, consequently, a single fixed point can be generated by each full circuit. In the nonlinear cases, phase space can be partitioned into different domains in which the circuits have the same types of eigenvalues. In such a domain, there is a fixed point with eigenvalues of the same type as those of the circuit under consideration. This circuit is functional and is responsible for the existence of this fixed point.

When partial circuits are considered, they are no longer associated with fixed points defined by setting $\dot{x}_i = 0$ for $i = 1, 2, 3$, but with points defined by setting $\dot{x}_i = 0$ for only one or two variables. In this work, we will only consider the case of partial circuits $J_{ij}J_{ji}$, which may be associated with a set of points defined by $\dot{x}_i = 0$ and $\dot{x}_j = 0$. There is a curve here called a double nullcline $\text{null}_{x_i} \cap \text{null}_{x_j}$, which may independently structure the phase portrait.

To end the introduction on feedback circuits, let us mention that the properties of negative and positive circuits are very different, as illustrated by the three conjectures proposed by Thomas [15]:

Conjecture 1. *The presence of a positive circuit in a given dynamical system is a necessary condition for multistationarity, that is, for the coexistence of two or more attractors in phase space.*

Conjecture 2. *The existence of a negative circuit (of two or more elements) is a necessary condition for oscillations (damped or sustained).*

Conjecture 3. *To generate chaotic behaviour, a system must have at least one positive and one negative circuit.*

3. Three simple chaotic systems

3.1. A first simple system

Sprott [19] recently proposed the simplest algebraic example of a dissipative jerk system. It consists of three terms including one quadratic nonlinearity. It reads

$$\dddot{x} = -a\ddot{x} + \dot{x}^2 - x. \tag{4}$$

This system can be rewritten as a set of three ordinary differential equations

$$\begin{cases} \dot{x} = y \\ \dot{y} = z \\ \dot{z} = -x + y^2 - az \end{cases} \tag{5}$$

where $y = \dot{x}$ and $z = \ddot{x}$. System (5) has a single fixed point F_0 located at the origin of the phase space. This is a saddle-focus SF_-. The Jacobian matrix is

$$J_{ij} = \begin{bmatrix} \cdot & 1 & \cdot \\ \cdot & \cdot & 1 \\ -1 & 2y & -a \end{bmatrix}. \tag{6}$$

This Jacobian matrix has a particular structure since only elements J_{12}, J_{23}, J_{31} ($i = 1, 2, 3$) are non-zero. Consequently, only the product $J_{12}J_{23}J_{31}$ is non-zero. There is thus a single full circuit which is indecomposable. This will be the case for the three systems investigated here. The full-circuit product $J_{12}J_{23}J_{31} = -1$ is constant and therefore is a non-ambiguous negative circuit. It can easily be checked that this full circuit is associated with the fixed point. It is therefore functional and relevant to the topology of the phase portrait.

In addition, the system has an ambiguous two-element circuit characterized by the product $J_{23}J_{32} = 2y$. This circuit is associated with the eigenvalues :

$$\lambda = \frac{-a \pm \sqrt{a^2 + 8y}}{2}. \tag{7}$$

The double nullcline $\mathrm{null}_y \cap \mathrm{null}_z$ defined by $x = y^2$ is made up of foci when $y < -\frac{a^2}{8}$ and of saddle otherwise. As developed in [16] this double nullcline is responsible for the local and global torsions identified in the attractor solution of system (5). The origin of these torsions will be detailed in the topological analysis described below. According to conjecture 3, co-existence between a positive circuit and a negative circuit is needed in order to generate chaotic behaviour. In this case, the negative circuit is required to have oscillations while co-existing with positive circuit $J_{23}J_{32}$ with $y > 0$. Nevertheless, the co-existence of two or more attractors has not been observed in this system.

When $a = 2.017\,05$, a chaotic attractor (figure 1) is obtained. This attractor is investigated using the Poincaré section

$$P_1 = \{(x_n, z_n) \in \mathbb{R}^2 \mid y_n = 0,\ \dot{y}_n < 0\}. \tag{8}$$

A bifurcation diagram (figure 2) is computed of x_n versus a within the interval ranging from $[2.017\,05; 2.13]$. Before the accumulation point occurring at $a = 2.0577$, the behaviour

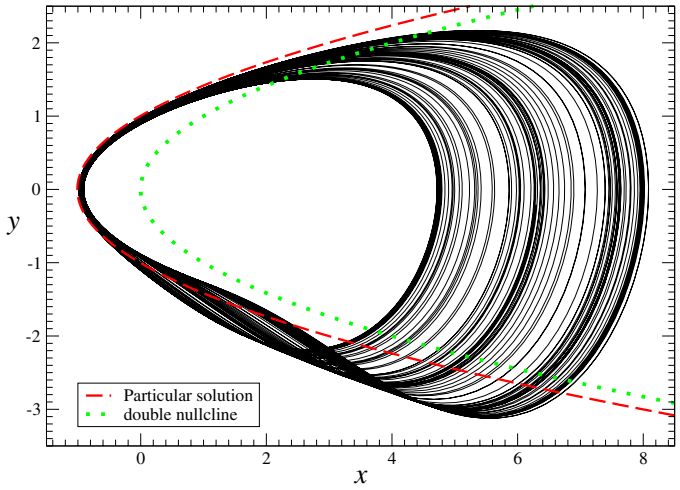

Figure 1. Chaotic attractor generated by system (5) just before the boundary crisis. The particular solution is drawn with a dashed line and the double nullcline $\text{null}_y \cap \text{null}_z$ with a dotted line ($a = 2.017\,05$).

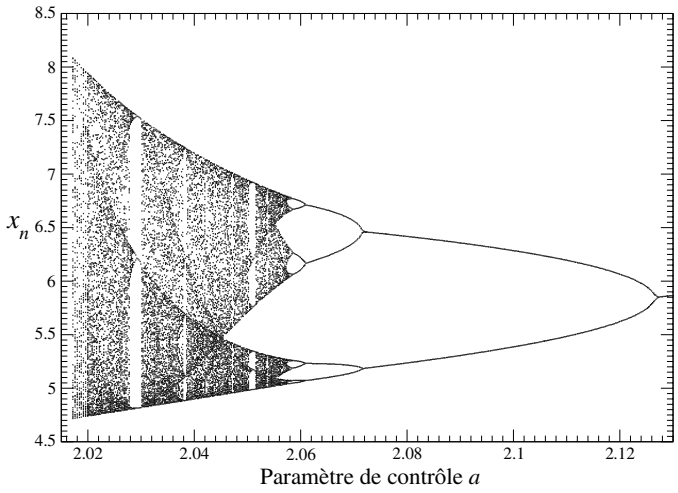

Figure 2. Bifurcation diagrams versus a for the simple jerk system (5).

becomes chaotic. Such a feature persists up to a boundary crisis when a is decreased. This crisis corresponds to the collision between the attractor and a particular solution of system (5) given by

$$x_P = \frac{t^2}{4} - \frac{a}{2} \tag{9}$$

where t is the time. This particular solution may be rewritten in the form

$$x_P = y^2 - \frac{a}{2} \tag{10}$$

Indeed, it can easily be checked in equation (4) that x_P is a particular solution. This analytical solution is shown in figure 1. Note that this particular solution has the same shape as the

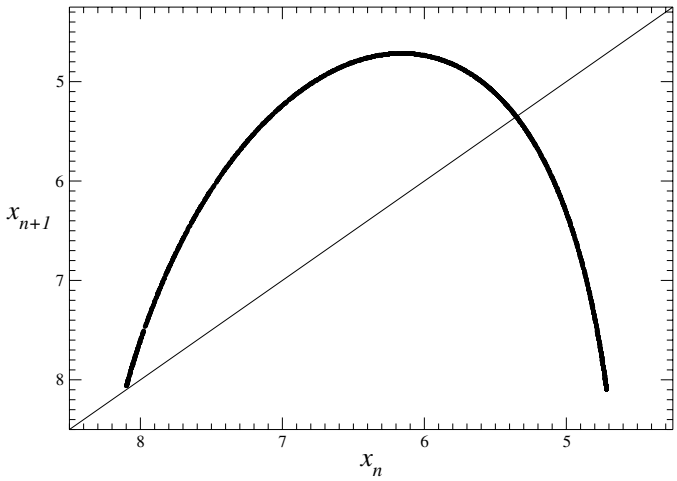

Figure 3. First-return map of the simple jerk system just before the boundary crisis ($a = 2.017\,05$). The increasing branch touches the bisecting line. This is a signature of a complete symbolic dynamics.

double nullcline $\text{null}_y \cap \text{null}_z$, but shifted by $-\frac{a}{2}$. In fact, the crisis appears when the attractor is characterized by a unimodal map for which the symbolic dynamics is complete, that is all periodic orbits which may be encoded using two symbols are embedded within the attractor [18]. Such a feature may be identified by computing the first-return map to the Poincaré section P_1 (figure 3). Within this interval for the a values, the bifurcation diagram can be predicted from the unimodal order [20]. The boundary crisis occurs for $a \approx 2.017\,05$. The behaviour is hereafter ejected to infinity. In fact, for slightly lower values of a, metastable chaotic behaviour is observed, that is the trajectory remains for a limited time in the neighbourhood of the unstable periodic orbits. After the metastable chaotic regime, the trajectory reaches the analytical solution (10) and is ejected to infinity. For instance, if a is set to 0.0168, varying initial conditions induce trajectories which make up to 300 cycles around the fixed point before being ejected to infinity.

Using the procedure described in [21, 22], a topological analysis of the chaotic attractor shown in figure 1 is performed. The unimodal map (figure 3) is constituted of two monotonic branches separated by a critical point. Consequently, the template synthesizing the topological properties of the attractor has two branches. Since an increasing (decreasing) branch of the first-return map is order preserving (reversing), the template must have one preserving branch with an even number of half-turns and one reversing branch with an odd number of half-turns. When no global torsion is identified, specifically when there are no global half-turns applied to both branches, a unimodal map as shown in figure 3 is associated with a so-called horseshoe template [22]. In the case of the attractor solution of system (5), one positive global torsion (one half-turn as drawn in figure 4) is identified in addition to the half-turn observed in one of the two branches of the attractor. This second half-turn is observed only in a single branch and is therefore called a local torsion. In the case of a trivial horseshoe template, the local torsion is associated with the decreasing branch of the map. In contrast to this, the local torsion here is conjugated with the global torsion (figure 4) and, thus, the branch with the local torsion undergoes two half-turns, making it order preserving. The local torsion is therefore associated with the increasing branch of the first-return map. For that reason, such a template is called a reverse horseshoe template. It is relevant to note that the local and global torsions are located

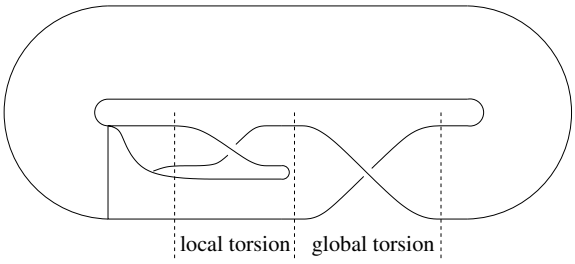

Figure 4. Reverse horseshoe template synthesizing the topological properties of the attractor generated by system (5). The increasing branch of the first-return map is associated with the branch with the local torsion.

in the neighbourhood of the double nullcline $\text{null}_y \cap \text{null}_z$, exactly where it is made up of focii. Such features strongly suggest that the double nullcline, identified using the feedback circuit analysis, is relevant for the topology of the chaotic attractor.

When the transformation

$$\begin{cases} x \mapsto \mu x \\ t \mapsto \lambda t \end{cases} \tag{11}$$

with the particular value $\mu = \lambda^2 = a$ is applied to equation (4), we obtain

$$\dddot{x} + \lambda^3(\ddot{x} - \dot{x}^2 + x) = 0. \tag{12}$$

When $\lambda \to \infty$ an asymptotic equation to system (5) may be written in the form

$$\ddot{x} - \dot{x}^2 + x = 0. \tag{13}$$

This asymptotic equation has a first integral. Setting $y = \dot{x}$, we have

$$yy' - y^2 + x = 0 \tag{14}$$

where $y' = \frac{\mathrm{d}y}{\mathrm{d}x}$. Since $yy' = \frac{1}{2}\frac{\mathrm{d}}{\mathrm{d}x}y^2$, the first integral

$$C = \left(y^2 - x - \frac{a}{2}\right)\mathrm{e}^{-\frac{2x}{a}} \tag{15}$$

is obtained using transformation (11). One has to note that the quantity in parentheses corresponds to particular solution (10). This first integral is drawn in figure 5 for different values of the constant C. The parabola associated with the particular solution ($C = 0$) is the boundary between the limit cycles which are solutions of the second-order differential equation (13) and solutions diverging to infinity. This parabola is the solution with which the attractor collides through a boundary crisis. Note that the fixed point is a centre for the asymptotic equation (13) while this is an unstable focus (restricted to the xy-plane) for system (5). The solutions for $C = 0$ correspond to the points located on the increasing branch of the first-return map shown in figure 3. These solutions touch the bisecting line, where a period-1 orbit should be located. This explains why the attractor is destroyed when the symbolic dynamics becomes complete. The other solutions do not correspond to any periodic orbit embedded within the attractor.

Note that the asymptotic equation is computed (after a rescaling) in the limit $a \to \infty$, while the chaotic attractor occurs for a restricted range of finite values of a. In fact, we are in a situation quite similar to the Schrödinger equation in the WKB approximation that strangely works very well, even when one puts $\hbar = 1$ in the numerical computation. However, this is also an asymptotic approximation that can suddenly give rise to a blowing up of the solution near what is called the turning points. In the case of system (5), the boundary plays this role.

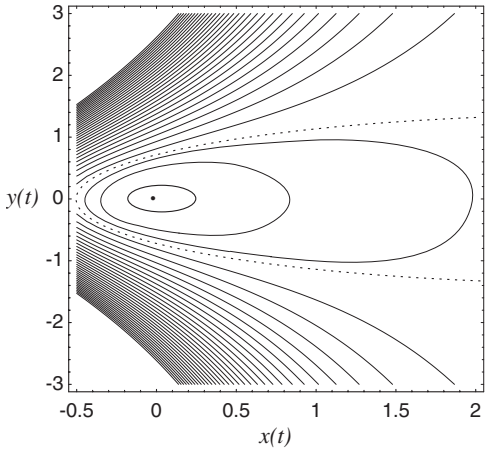

Figure 5. Phase portrait of the asymptotic equation (13) of system (5) for different values of the constant C. The boundary ($C = 0$) is drawn with a dashed line. Parameter value: $a = 2.1$.

3.2. A second simple chaotic system

By modifying the third-order differential equation (4), Sprott obtained

$$\dddot{x} = -a\ddot{x} + \dot{x}x - x \tag{16}$$

which may be rewritten in the form

$$\begin{cases} \dot{x} = y \\ \dot{y} = z \\ \dot{z} = -x + xy - az. \end{cases} \tag{17}$$

This system has a single fixed point F_0 which is also a saddle-focus SF_-. It is located at the origin of the phase space. The single full circuit associated with the product $J_{12}J_{23}J_{31} = y - 1$ is ambiguous. At the fixed point, that is for $y = 0$, the full circuit is negative ($J_{12}J_{23}J_{31} = -1$) and is characterized by the same eigenvalues as for system (5). There is also a partial circuit associated with the product $J_{23}J_{32} = x$ which is ambiguous. The corresponding double nullcline $\mathrm{null}_y \cap \mathrm{null}_z$ is defined by $y = 1$ in the plane $z = 0$, and the associated eigenvalues are $\lambda_\pm = \frac{-a \pm \sqrt{a^2+4x}}{2}$. This double nullcline is therefore a line made of foci when $x < -\frac{a^2}{4}$ and saddles for $x > -\frac{a^2}{4}$. As for system (5), the local and global torsions which may be identified in this attractor are located in the neighbourhood of the double nullcline $\mathrm{null}_y \cap \mathrm{null}_z$ (figure 6) where its points are foci. The ambiguity of the full circuit could be sufficient to allow the existence of chaotic behaviour since it is negative for $y < 1$, and positive otherwise. The domain over which the circuit $J_{12}J_{23}J_{31}$ is negative is clearly responsible for the existence of oscillations. This is because the circuit is associated with the fixed points around which the attractor is structured. Thus, the two-element circuit $J_{23}J_{32}$ is relevant to structure the phase portrait in the domain in which it is positive ($x > 0$). The negative contribution of full circuit $J_{12}J_{23}J_{31}$ and the positive contribution of the two-element circuit $J_{23}J_{32}$ induce the possible existence of chaotic behaviour according to conjecture 3. As for the previous system, the co-existence of attractors has not been observed.

A chaotic attractor is obtained when setting the control parameter a to 2.017 05 (figure 6). Using the Poincaré section

$$P_2 = \{(x_n, z_n) \in \mathbb{R}^2 \mid y_n = 0, \dot{y}_n > 0\} \tag{18}$$

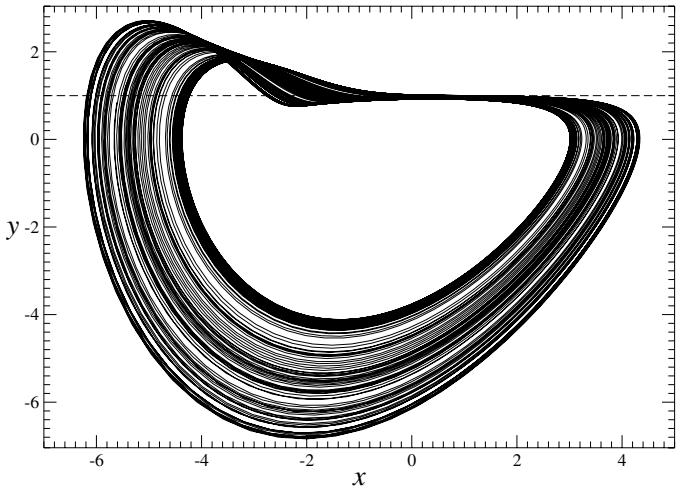

Figure 6. Chaotic attractor generated by the simple jerk system just before the boundary crisis with the particular solution drawn with a dashed line. The topology of this attractor is also characterized by a reverse horseshoe template but with negative half-turns. This is irrelevant since a permutation between two coordinates, say y and z, inverses the sign of rotation ($a = 2.017\,05$).

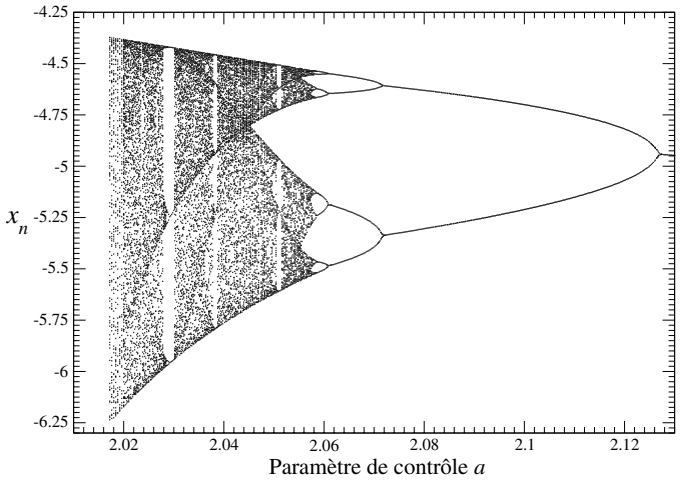

Figure 7. Bifurcation diagram versus a for the simple jerk dynamics (17).

a bifurcation diagram (figure 7) is computed for a range of a between 2.0168 and 2.13. This interval is the same as in system (5). After the accumulation point in which $a < 2.0577$, the behaviour is chaotic. The corresponding attractor exists up to a boundary crisis occurring at $a = 2.017\,05$. Similarly to system (5), the attractor collides with the particular solution of equation (16) reading as $x = t$. Such particular solution may be rewritten in the form $y = 1$ (figure 6). In this case, the particular solution is also the double nullcline $\text{null}_y \cap \text{null}_z$. It may easily be checked that the bifurcation diagram of system (17) (figure 7) is equivalent to that of system (5) (figure 2). In particular, the boundary crisis also occurs when the symbolic dynamics is complete as evidenced by the first-return map computed for $a = 2.017\,05$ (figure 8). A topological analysis reveals that periodic orbits embedded within the attractor

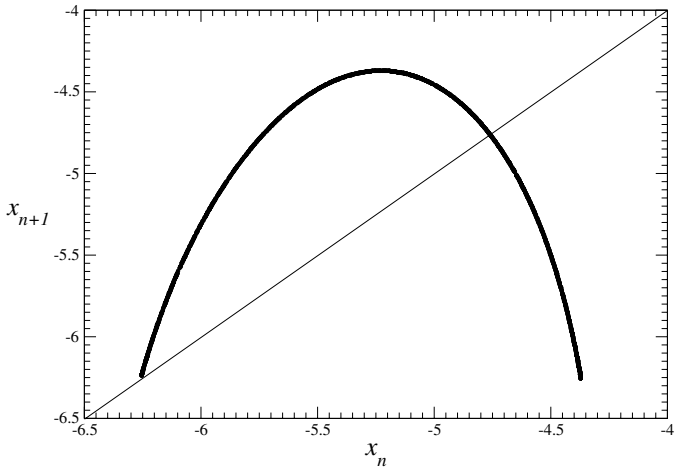

Figure 8. First-return map of the simple jerk system just before the boundary crisis ($a = 2.017\,05$).

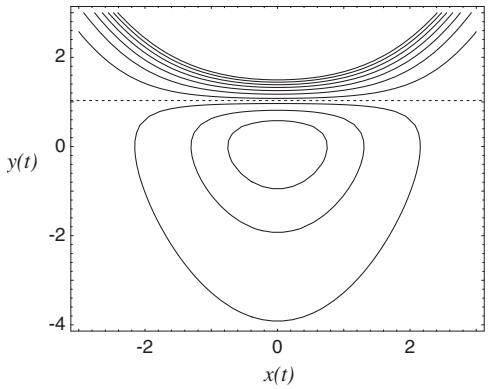

Figure 9. Phase portrait of the asymptotic equation (19) of system (17) for different values of the constant C. The boundary ($C = 0$) is drawn with a dashed line. Parameter value: 2.1.

are organized according to the template associated with the attractor of system (5). Thus, this is a horseshoe template as suggested by the first-return map which looks like a parabola. A global torsion is also observed in the attractor (left upper part of the attractor shown in figure 8). The attractors of systems (5) and (17) are therefore topologically equivalent. For both systems, the nullcline $\text{null}_y \cap \text{null}_z$ is responsible for the global and local torsion. The attractors therefore result from the full circuit responsible for the existence of the fixed point and the two-element circuit inducing the torsion.

Similarly to system (5), the asymptotic equation

$$\ddot{x} - x\dot{x} + x = 0 \tag{19}$$

may be obtained using transformation (11) but with the values ($a = \mu^2 = \lambda^2$). Such an asymptotic equation has the first integral

$$C = (y - 1)\exp\left(y - \frac{x^2}{2a}\right). \tag{20}$$

This integral is shown for different values of the constant C (figure 9). Again, the particular solution ($C = 0$) is the boundary between the limit cycle ($C < 0$) and the solutions diverging to infinity ($C > 0$). As for the previous system, the solution with $C = 0$ corresponds to the period-1 orbit located at the intersection of the increasing branch of the first-return map (figure 8) and the bisecting line.

Additional analytical computations may be done. Using the transformation $x \mapsto t + x_0 + u$ where x_0 is a constant and u is a perturbed solution searched near the particular solution $x = t$, the third-order differential equation (16) becomes

$$\dddot{u} + a\ddot{u} - (t + x_0)\dot{u} - u\dot{u} = 0. \tag{21}$$

In order to obtain a perturbed solution, the term $u\dot{u}$ has to be neglected. Setting $w = \dot{u}$, the linear second-order differential equation

$$\ddot{w} + a\dot{w} - (t + x_0)w = 0 \tag{22}$$

is obtained. Assuming that $w = W\,\mathrm{e}^{-at/2}$, we obtain

$$\ddot{W} - \left(t + x_0 + \frac{a^2}{4}\right) W = 0. \tag{23}$$

Analytical solutions to this equation depend on Airy functions. They are

$$w = \dot{u} = \exp(-at/2)\,[\alpha Ai(\tau) + \beta Bi(\tau)] \tag{24}$$

where we put $\tau = t + x_0 + a^2/4$, and where α and β are integration constants. Thus, x is given by

$$x = t + x_0 + \int_0^t w(t')\,\mathrm{d}t'. \tag{25}$$

To have a perturbed solution $w(t)$, initial conditions cancelling the integration constant β must be chosen since the function Bi tends towards infinity when $t \to \infty$. Choosing initial conditions, $x = x_0$, $\dot{x} = y_0 \neq 1$ and $\ddot{x} = 0$, we find

$$\beta = \pi(y_0 - 1)\left(\frac{a}{2}Ai(x_0 + a^2/4) - Ai'(x_0 + a^2/4)\right) = 0. \tag{26}$$

The initial condition $y_0 = 1$ has not been retained because it induces the trivial solution. There exists a countable infinite set of values x_0 for a given a, leading to $\beta = 0$, which are related to the zeros of the Airy function. For any values of a corresponding to the chaotic regime, the perturbed solution may be found as close as possible to the particular solution $x = t$ which belongs to the attractor!

3.3. The simplest equivariant jerk system

Symmetries have always played an important role in physics, from fundamental formulations of basic principles to concrete applications. Symmetries are also present in a variety of chaotic systems. Among them is the well-known Lorenz system [3] which has a rotation symmetry. The simplest jerk system with symmetry properties was proposed by Malasoma [11] and reads as

$$\begin{cases} \dot{x} = y \\ \dot{y} = z \\ \dot{z} = -az + xy^2 - x. \end{cases} \tag{27}$$

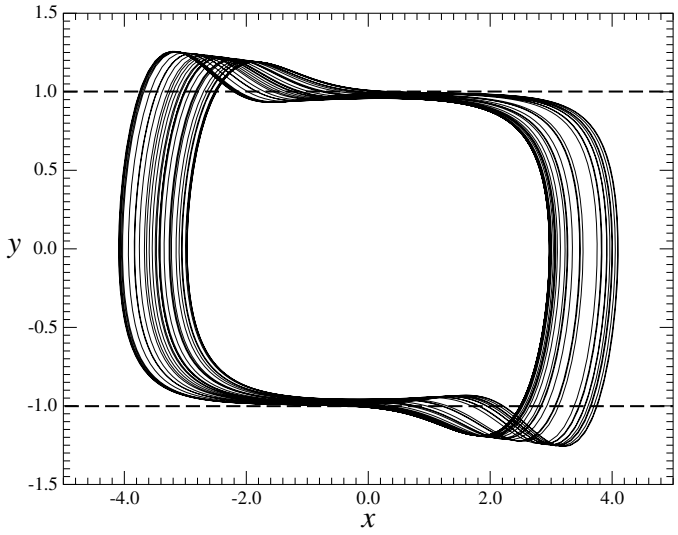

Figure 10. Chaotic attractor generated by the simplest equivariant jerk system just before the boundary crisis ($\alpha = 2.027\,717$). The particular solutions $y = \pm 1$ are drawn with dashed lines. They correspond to the double nullclines $\text{null}_y \cap \text{null}_z$.

This system is equivariant in that it obeys the relation $\gamma \cdot \boldsymbol{f}(\boldsymbol{x}) = \boldsymbol{f}(\gamma \cdot \boldsymbol{x})$ where γ is a 3×3 matrix defining the symmetry properties. In the present case, the γ-matrix

$$\gamma = \begin{bmatrix} -1 & 0 & 0 \\ 0 & -1 & 0 \\ 0 & 0 & -1 \end{bmatrix} \tag{28}$$

defines an inversion symmetry $\mathcal{P}$. It means that the vector field $\boldsymbol{f}$ is invariant when (x, y, z) are mapped into $(-x, -y, -z)$. System (5) has a single fixed point F_0 located at the origin of the phase space. This is a saddle-focus SF_-.

The single full circuit is associated with $J_{12}J_{23}J_{31} = y^2 - 1$ and is *ambiguous*. The fixed point F_0 is located in the domain of phase space where the full circuit is negative ($|y| < 1$). This is in agreement with the fact that it is a saddle-focus characterized by a negative real eigenvalue. The full circuit is therefore functional in the domain $|y| < 1$ where it is negative. It is thus responsible for the existence of oscillations as suggested by conjecture 1. There is also a two-element circuit associated with $J_{23}J_{32} = 2xy$. The corresponding double nullcline $\text{null}_y \cap \text{null}_z$ is defined by $y = \pm 1$. The associated eigenvalues are

$$\lambda = \frac{-a \pm \sqrt{a^2 + 8xy}}{2}. \tag{29}$$

The double nullclines $y = \pm 1$ are made of stable foci when $x < -\frac{a^2}{8}$ (resp. $x > \frac{a^2}{8}$) and saddles otherwise. The symmetry properties are therefore recovered in the structure of the double nullclines. Again, the local and global torsion are located in the neighbourhood of the segments of the double nullclines made of points with complex eigenvalues. As for system (27), the two-element circuit $J_{23}J_{32}$ is positive for $xy > 0$. It contributes to the co-existence of two attractors observed with $a > 2.0644$ as detailed below. The co-existence of the negative full circuit and the positive two-element circuit satisfies the conditions for conjecture 3 for chaotic attractors. Note that the product xy matches the symmetry properties of the attractor.

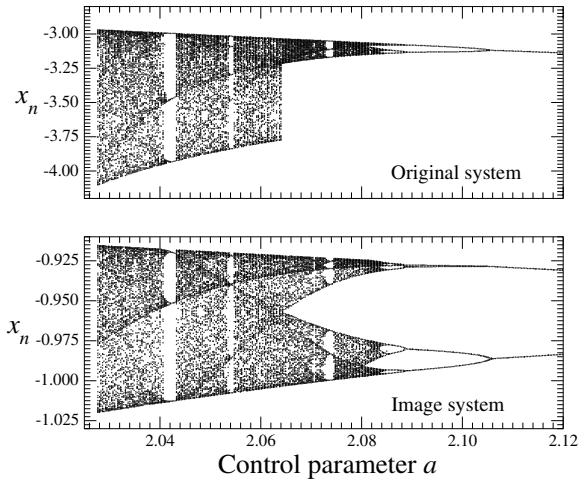

Figure 11. Bifurcation diagram versus a of the simplest equivariant jerk dynamics (27). The bifurcation diagram for its image is also shown.

When $a = 2.027\,717$ and the initial conditions are $(x_0, y_0, z_0) = (4.0, 0.0, 0.0)$, the chaotic attractor shown in figure 10 is obtained. The attractor exhibits a symmetry around the Oz-axis under the action of γ. This attractor is investigated using the Poincaré section

$$P_O = \{(x_n, z_n) \in \mathbb{R}^2 \mid y_n = 0, \dot{y}_n < 0\}. \tag{30}$$

A bifurcation diagram (figure 11) is computed versus a within the interval $[2.027\,717; 2.2]$. When a is decreased, two simultaneous period-doubling cascades are observed. The two cascades are symmetric under the action of γ. Only one of these cascades is shown in figure 11(a). After the accumulation point for $a = 2.0840$, the behaviour becomes chaotic. Depending on the initial conditions, two attractors which are symmetric under the action of γ are observed. Such a feature persists up to an attractor merging crisis. This crisis corresponds to the sudden increase in size of the chaotic attractor and results from two attractors which collide to form a single symmetric attractor [23]. In fact, the crisis occurs when each attractor is characterized by a unimodal map for which the symbolic dynamics is complete. For $a \in]2.0644; 2.2]$, the bifurcation diagram can be predicted from the unimodal order [20]. The attractor merging crisis occurs for $a \approx 2.0644$. For values smaller than a, a single attractor which is globally invariant under the action of γ is observed (as well exemplified in figure 10).

When $a < 2.0644$, the single symmetric chaotic attractor is characterized by a multimodal map which may have up to three critical points. Such a map can be observed for a value of $a = 2.027\,717$ [24]. In that case, the bifurcation diagram can no longer be predicted by kneading theory. When more than one critical point is involved through a variation of a control parameter, there is no longer universal order for the creation/destruction of periodic orbits.

Nevertheless, when an equivariant system is considered, it may be possible to simplify the analysis by modding out the symmetry properties. Such a procedure was initially introduced by mapping the dynamics in a fundamental domain of the phase space [18]. Recently it was developed by using the image of equivariant systems [25], which results from the $2 \to 1$ mapping of the equivariant system to obtain a projection of the dynamics without any residual symmetry. The dynamical system (5) which is invariant under the inversion symmetry is

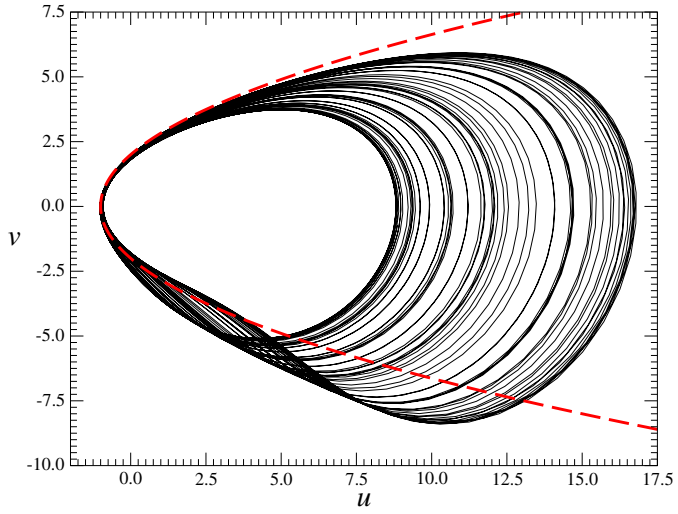

Figure 12. Image of the simplest equivariant jerk system just before the boundary crisis. A reverse horseshoe template describes the topological properties of this attractor ($a = 2.027\,717$).

thus mapped into a locally equivalent dynamical system. This is done by constructing a nonlinear coordinate transformation $(x, y, z) \to (u, v, w)$ in which the coordinates (u, v, w) are invariant under the inversion symmetry $\mathcal{P}$. The elementary polynomials in (x, y, z) of degree up to two, and invariant under $\mathcal{P}$, are xy, yz, zx, x^2, y^2 and z^2. The following coordinate transformation is convenient [24] :

$$\varphi = \begin{vmatrix} u = x^2 - y^2 \\ v = 2xy \\ w = z^2. \end{vmatrix} \tag{31}$$

The invariant dynamical system equation $\dot{u}_i = g_i(\boldsymbol{u})$ where $\boldsymbol{u} = (u_1 = u, u_2 = v, u_3 = w)$ are determined in a straightforward way

$$\dot{u}_i = \frac{\partial u_i}{\partial x_j}\frac{\mathrm{d}x_j}{\mathrm{d}t} = \frac{\partial u_i}{\partial x_j}F_j(\boldsymbol{x}) = g_i(\boldsymbol{u}). \tag{32}$$

Using $2x^2 = \rho + u$ and $2y^2 = \rho - u$ where $\rho = \sqrt{u^2 + v^2}$, the invariant equations of system (27) are

$$\begin{cases} \dot{u} = v \pm \sqrt{(\rho - u)w} \\ \dot{v} = \rho - u \pm \sqrt{(\rho - u)w} \\ \dot{w} = -2aw \pm \left[\frac{\rho - u}{2} - 1\right]\sqrt{(\rho + u)w}. \end{cases} \tag{33}$$

The image attractor (figure 12) can also be obtained by applying the map φ onto the original attractor. No residual symmetry can be identified in the resulting system.

The image attractor is investigated using the Poincaré section

$$P_I = \{(u_n, w_n) \in \mathbb{R}^2 \,|\, v_n = 0, \dot{v}_n < 0\}. \tag{34}$$

Since the Poincaré section is unidimensional, a first-return map may be built with a single variable to define the partition of the attractor. For $a = 2.027\,717$ (figure 13), the map is unimodal and its increasing branch touches the bisecting line. The symbolic dynamics is thus complete. A mapping of a four branch first-return map into a unimodal map has already

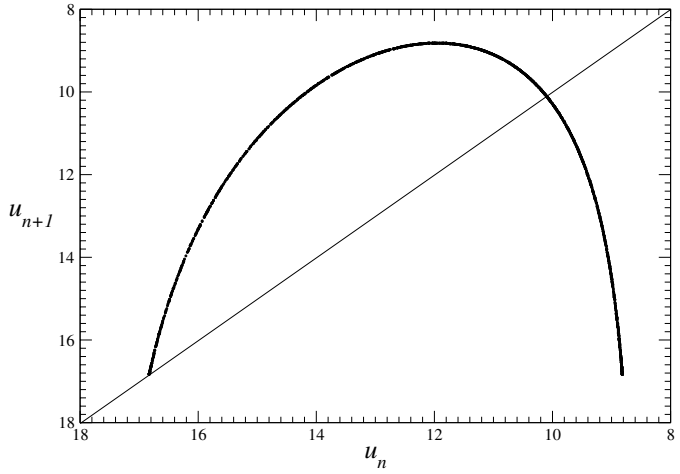

Figure 13. First-return map of the image system of the simplest equivariant jerk system just before the boundary crisis ($a = 2.027\,717$). A similar map may be obtained using the w-variable.

been observed in the Burke and Shaw system when the symmetry is modded out [18]. This was investigated for the simplest jerk equivariant system in [24]. This image attractor is characterized by the reverse horseshoe template (figure 4) exhibited for the previous two systems. The image attractor is therefore topologically equivalent to the attractor solution of systems (5) and (17). The bifurcation diagram (figure 11(b)) of the image system is typical of a unimodal map with a differentiable maximum. As detailed for the Burke and Shaw system [18], a period-1 orbit in the original system becomes a period-2 orbit in the image system as easily observed for $a = 2.11$ in figure 11.

The attractor in the original phase space $\mathbb{R}^3(x, y, z)$ disappears through a boundary crisis for a-values slightly smaller. Such a feature occurs when the attractor collides with the two double nullclines (figure 10). This is a scenario similar to that encountered for the two previous systems. The particular solutions $y = \pm 1$ are mapped under the $2 \to 1$ map φ, into a single solution defined by $u = \frac{v^2}{4} - 1$ shown in figure 12. In the image space $\mathbb{R}^3(u, v, w)$, we recover exactly the shape of the attractor (figure 1) generated by system (5) with its particular solution. From this point of view, all three systems belong to a class of equivalence since a nonlinear coordinate transformation allows us to switch from one representation to another. Note that from a feedback circuit analysis, these three systems have a similar structure, modulo the symmetry properties.

An asymptotic equation may be obtained as for the previous cases. A first integral

$$C = (y^2 - 1) \exp\left(-\frac{x^2}{a}\right) \tag{35}$$

is thus obtained (figure 14). Again, the separatrices correspond to the particular solutions of system (27). A perturbed solution can also be searched around particular solutions using

$$x(t) = \pm t + x_0 + u. \tag{36}$$

In order to obtain this perturbed solution, the equation

$$\dddot{u} + a\ddot{u} - 2(t \pm x_0)\dot{u} = 0 \tag{37}$$

must be solved. We have to distinguish the two cases $\pm x_0$. Again, putting $w = \dot{u}$, we readily obtain an equation that can be mapped with a scaling to equation (23). So the solutions

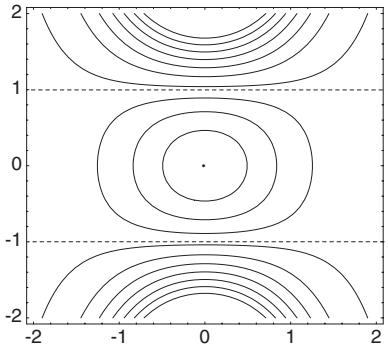

Figure 14. Phase portrait of the asymptotic equation of system (27) for different values of the constant C. The boundary ($C = 0$) is drawn with dashed lines. Parameter value: $a = 2.1$.

may be expressed in terms of Airy functions leading to similar conclusions, that is to say particular solutions with $C = 0$ belong to the attractor when the first-return map has a branch which touches the bisecting line. This intersection point induces the boundary crisis and, consequently, the ejection of the trajectory to infinity.

4. Conclusion

Three simple systems generating chaotic behaviour have been investigated. Particular solutions have been found for each of them. In all cases, these particular solutions are responsible for the destruction of the chaotic attractor through a boundary crisis in which the attractors collide with particular solutions. By using a feedback analysis, it has been shown that all attractors are structured around a single fixed point located at the origin of the phase space. The first two attractors without any symmetry properties are also structured around one double nullcline made of foci in the neighbourhood of the global torsion and the local torsion. These torsions may be identified. In the case of the simplest equivariant system, there are two double nullclines, one being a symmetry of the other. When the symmetry properties are modded out using a $2 \rightarrow 1$ mapping, the image attractor obtained is topologically equivalent to the attractor of the first two systems investigated. Through this, we may conjecture that the three systems belong to a single class of systems. From the feedback circuit structures, this is quite obvious since all of them have a full circuit and a two-element circuit associated with double nullclines structuring the attractor. Moreover, the attractors of the two systems without any symmetry properties and the image attractor of the equivariant system are topologically equivalent, thus providing a first link between the feedback circuit structure of the equations and the topological properties of their attractors.

Acknowledgments

CL wishes to thank René Thomas and Marcelle Kaufman for helpful discussions on the description of dynamical systems with feedback circuits. We thank Greg Byrne for helping us to improve the English.

References

[1] Poincaré H 1899 *Les méthodes nouvelles de la Mécanique céleste* vol III (Paris: Gauthier-Villars)
[2] Bendixson I 1901 Sur les courbes définies par des équations différentielles *Acta Math.* **24** 1–88
[3] Lorenz E N 1963 Deterministic nonperiodic flow *J. Atmospheric Sci.* **20** 130–41
[4] Rössler O E 1976 An equation for continuous chaos *Phys. Lett.* A **57** 397–8
[5] Rössler O E 1979 Continous chaos—four prototype equations *Ann. NY Acad. Sci.* **316** 376–92
[6] Sprott J C 1994 Some simple chaotic flows *Phys. Rev.* E **50** 647–50
[7] Gottlieb H P W 1996 What is the simplest jerk function that gives chaos? *Am. J. Phys.* **64** 525
[8] Gouesbet G and Letellier C 1994 Global vector field reconstruction by using a multivariate polynomial L_2-approximation on nets *Phys. Rev.* E **49** 4955–72
[9] Linz S J 1997 Nonlinear dynamical models and jerky motion *Am. J. Phys.* **65** 523–43
[10] Fu Z and Heidel J 1997 Non chaotic behaviour in three-dimensional quadratic systems *Nonlinearity* **10** 1289–303
[11] Malasoma J-M 2000 What is the simplest dissipative chaotic jerk equation which is parity invariant ? *Phys. Lett.* A **264** 383–9
[12] Thomas R 1984 Logical description, analysis and synthesis of biological and other networks comprising feedback loops *Adv. Chem. Phys.* **55** 247–82
[13] Thomas R 1981 On the relation between the logical structure of systems and their ability to generate multiple steady states or sustained oscillations *Springer Ser. Synerg.* **9** 180–93
[14] Thomas R and Kaufman M 2001 Multistationarity, the basis of cell differentiation and memory: I. Structural conditions of multistationarity and other nontrivial behaviour *Chaos* **11** 170–9
[15] Thomas R 1999 Deterministic chaos seen in terms of feedback circuits: analysis, synthesis, 'labyrinth chaos' *Int. J. Bifurcations Chaos* **9** 1889–905
[16] Letellier C, Thomas R and Kaufman M 2003 Classification of dynamical systems using feedback circuit, submitted
[17] Snoussi El H and Thomas R 1993 Logical identification of all steady states: the concept of feedback loop characteristic states *Bull. Math. Biol.* **55** 973–91
[18] Letellier C, Dutertre P, Reizner J and Gouesbet G 1996 Evolution of multimodal map induced by an equivariant vector field *J. Phys. A: Math. Gen.* **29** 5359–73
[19] Sprott J C and Linz S J 2000 Algebraically simple chaotic flows *Int. J. Chaos Theory Appl.* **5** 3–22
[20] Collet P and Eckmann J P 1980 Iterated maps on the interval as dynamical systems *Progress in Physics* ed A Jaffe and D Ruelle (Boston, MA: Birkhäuser)
[21] Letellier C, Dutertre P and Maheu B 1995 Unstable periodic orbits and templates of the Rössler system: toward a systematic topological characterization *Chaos* **5** 271–82
[22] Gilmore R 1998 Topological analysis of chaotic dynamical systems *Rev. Mod. Phys.* **70** 1455–529
[23] Ott E 1993 *Chaos in Dynamical System* (Cambridge: Cambridge University Press)
[24] Letellier C and Malasoma J-M 2001 Unimodal order in the image of the simplest equivariant jerk system *Phys. Rev.* E **64** 067202
[25] Letellier C and Gilmore R 2001 Covering dynamical systems: two-fold covers *Phys. Rev.* E **63** 16206